Proceedings of the 29th Polish-Slovak Scientific Conference on Machine Modelling and Simulations 2024, Poland

Numerical Modeling of the Bronze Solidification Process with Consideration of the Influence of an Air Gap Between the Mold and the Casting

T. Skrzypczak* and L. Sowa

Czestochowa University of Technology, Faculty of Mechanical Engineering, 42-201 Częstochowa, Poland

Doi: 10.12693/APhysPolA.145.743 *e-mail: tomasz.skrzypczak@pcz.pl

The presented work shows the results of numerical modeling of the bronze solidification process in a permanent mold made of cast iron in a three-dimensional space, incorporating thermophysical phenomena. The model considers the effect of the air gap between the mold and the casting, which has a variable width, on the rate of the solidification process. Employing the finite element method with independent spatial discretization of the casting and the mold, the model accounts for the thermal deformations of the casting, while the mold is assumed to be undeformable. This approach involves the use of two separate meshes to obtain temporary temperature fields as well as deformations. The thermal interaction between the bronze casting and the mold is described by appropriate boundary conditions. The solution is obtained sequentially at each time step independently for each volume.

topics: numerical modeling, finite element method (FEM), solidification process, heat transfer

1. Introduction

The casting solidification process involves various physical phenomena such as heat transfer, fluid flow, and phase changes. The quality of the manufactured object depends on controlling and optimizing this process. The air gap between the mold and the casting, formed due to metal shrinkage during cooling, acts as thermal resistance, affecting heat transfer, solidification time, and the risk of defects. Numerical models, based on conservation equations for mass, momentum, energy, and species, help predict the solidification process, incorporating methods to track the solid–liquid interface and air gap width. Different boundary conditions simulate various casting scenarios, such as mold cooling and electromagnetic stirring.

Several studies highlight the importance of air gap formation and its impact on heat transfer and microstructure formation. Mortensen et al. [1] studied air gap formation during aluminum casting, while other researchers examined the effects of mold material properties [2], measured air gap formation in steel-ingot casting [3], and simulated directional solidification processes [4]. Chawla et al. [5] focused on the horizontal continuous casting of cast iron, analyzing the effect of air gap on the solidification process.

This work models the variable air gap size between bronze casting and permanent mold using finite element method (FEM) with separate spatial discretization for both components. Thermally dependent volume changes and resulting displacements are considered. Two separate meshes are used to obtain temperature fields, with boundary conditions describing thermal interactions. A novel method is applied to calculate the air gap width at each time step based on local distances between surfaces in thermal contact, enhancing previous approaches like those in [6] for two-dimensional problems.

2. Mathematical and numerical models

Figure 1 shows a schematic of the problem, with the region divided into two volumes, i.e., Ω_M (the cast iron mold) and Ω_C (the solidifying bronze). During the liquid–solid transition, the heat transport during solidification causes thermal deformations of the casting, while the mold is assumed to be non-deformable. This assumption leads to the creation of a gap between boundaries Γ_M and Γ_C. The gap width, h, changes with temperature variations in the casting. Heat transfer from the casting to the mold is affected by the thermal resistance of the gap. Heat is also transferred to the outside

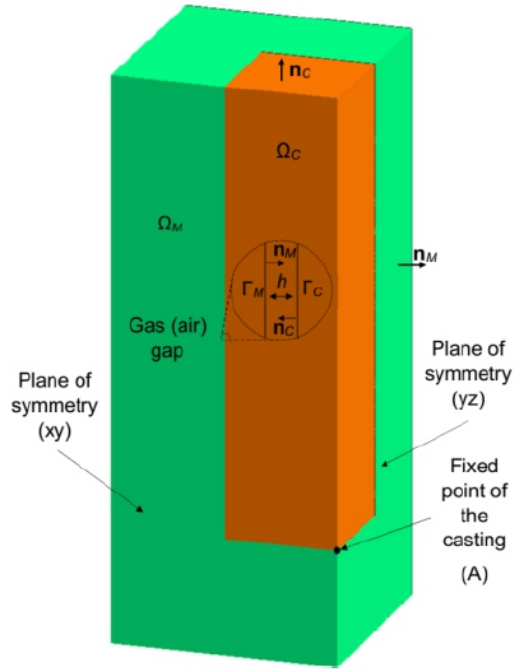

Fig. 1. Mold-casting system with an air gap.

through the external surfaces due to the lower ambient temperature. Air in the gap influences heat transport characteristics. The model ignores gravity forces, mechanical loads, and shrinkage during the phase change. Due to symmetry, only a quarter of the mold-casting system is taken into account. Thermal insulation is assumed on the xy and yz planes of symmetry. Additionally, the following displacement conditions are applied: $z = 0$ on the xy plane, $x = 0$ on the yz plane, and $x = y = z = 0$ at the fixed point A.

To describe the thermomechanical behavior of the mold-casting system, the following governing equations are used

$$\frac{\partial}{\partial x}\left(\lambda_{(i)}\frac{\partial T^{(i)}}{\partial x}\right)+\frac{\partial}{\partial y}\left(\lambda_{(i)}\frac{\partial T^{(i)}}{\partial y}\right)+\frac{\partial}{\partial z}\left(\lambda_{(i)}\frac{\partial T^{(i)}}{\partial z}\right)=c_{(i)}\rho_{(i)}\frac{\partial T^{(i)}}{\partial t}, \tag{1}$$

$$\begin{aligned}\frac{\partial \sigma_x^{(i)}}{\partial x}+\frac{\partial \tau_{xy}^{(i)}}{\partial y}+\frac{\partial \tau_{xz}^{(i)}}{\partial z}&=0,\\ \frac{\partial \tau_{xy}^{(i)}}{\partial x}+\frac{\partial \sigma_y^{(i)}}{\partial y}+\frac{\partial \tau_{yz}^{(i)}}{\partial z}&=0,\\ \frac{\partial \tau_{xz}^{(i)}}{\partial x}+\frac{\partial \tau_{yz}^{(i)}}{\partial y}+\frac{\partial \sigma_z^{(i)}}{\partial z}&=0.\end{aligned} \tag{2}$$

The variables used in the model include: thermal conductivity coefficient λ [J/(s m K)], specific heat capacity c [J/(K kg)], density ρ [kg/m^3], temperature T [K], components of the symmetrical stress tensor σ_x, σ_y, σ_z, τ_{xy}, τ_{xz}, τ_{yz} [N/m^2], time t [s], Cartesian coordinates x, y, z [m], and the index i, which denotes the i-th volume. Here, the index i specifically refers to either the casting (C) or the mold (M). The initial and boundary conditions for (1) are as follows

$$T^{(C)}(x,y,z,0)=T_0^{(C)},\quad T^{(M)}(x,y,z,0)=T_0^{(M)}, \tag{3}$$

$$-\lambda_C\frac{\partial T^{(C)}}{\partial n_C}=\frac{\lambda_g}{h}\left(T_b^{(C)}-T_b^{(M)}\right)=\lambda_M\frac{\partial T^{(M)}}{\partial n_M}, \tag{4}$$

$$\begin{aligned}-\lambda_C\frac{\partial T^{(C)}}{\partial n_C}&=\alpha_C\left(T^{(C)}-T_{amb}^{(C)}\right),\\ -\lambda_M\frac{\partial T^{(M)}}{\partial n_M}&=\alpha_M\left(T^{(M)}-T_{amb}^{(M)}\right).\end{aligned} \tag{5}$$

The local gap width is denoted by h [m], and the local normal vectors to the boundaries Γ_C and Γ_M are represented by $\boldsymbol{n}_C$ and $\boldsymbol{n}_M$, respectively. In (3)–(5), $T_b^{(C)}$ and $T_b^{(M)}$ [K] indicate the local temperatures of the volumes Ω_C and Ω_M at the contact boundaries, while $T_0^{(C)}$ and $T_0^{(M)}$ [K] are the initial temperatures of these volumes; $T^{(C)}$ and $T^{(M)}$ [K] represent the local temperatures of Ω_C and Ω_M at the external boundaries; $T_{amb}^{(C)}$ and $T_{amb}^{(M)}$ [K] are the ambient temperatures outside the casting and the mold, while α_C and α_M [J/(s m^2 K)] are the heat convection coefficients at the external boundaries. Finally, λ_g denotes the thermal conductivity of the medium filling the gap. The calculation of the heat capacity in the casting can be performed using the following relations

$$c_C=\begin{cases}c_s, & T^{(C)}<T_S,\\ \frac{(c_s+c_l)}{2}+\frac{L}{T_L-T_S}, & T_S\le T^{(C)}\le T_L,\\ c_l, & T^{(C)}>T_L,\end{cases} \tag{6}$$

where T_L and T_S [K] are the liquidus and solidus temperatures, c_s and c_l [J/(kg K)] indicate the specific heat capacities of the solid and liquid phases of the casting, and L [J/kg] is the latent heat of solidification.

It should be noted that (2) contains six unknowns, which must be transformed into the functions of displacements using appropriate strain–stress and strain–displacement relations [6]. The final form of these equations is as follows

$$f_4 a_{(i)}\Delta T^{(i)}+f_1\frac{\partial^2 u_x^{(i)}}{\partial x^2}+f_2\left(\frac{\partial^2 u_y^{(i)}}{\partial x\partial y}+\frac{\partial^2 u_z^{(i)}}{\partial x\partial z}\right)+f_3\left(\frac{\partial^2 u_x^{(i)}}{\partial y^2}+\frac{\partial^2 u_x^{(i)}}{\partial z^2}+\frac{\partial^2 u_y^{(i)}}{\partial y\partial x}+\frac{\partial^2 u_z^{(i)}}{\partial z\partial x}\right)=0, \tag{7}$$

$$f_4 a_{(i)}\Delta T^{(i)}+f_1\frac{\partial^2 u_y^{(i)}}{\partial y^2}+f_2\left(\frac{\partial^2 u_x^{(i)}}{\partial y\partial x}+\frac{\partial^2 u_z^{(i)}}{\partial y\partial z}\right)+f_3\left(\frac{\partial^2 u_x^{(i)}}{\partial x\partial y}+\frac{\partial^2 u_y^{(i)}}{\partial x^2}+\frac{\partial^2 u_y^{(i)}}{\partial z^2}+\frac{\partial^2 u_z^{(i)}}{\partial z\partial y}\right)=0, \tag{8}$$

$$f_4 a_{(i)} \Delta T^{(i)} + f_1 \frac{\partial^2 u_z^{(i)}}{\partial z^2} + f_2 \left(\frac{\partial^2 u_x^{(i)}}{\partial z \partial x} + \frac{\partial^2 u_y^{(i)}}{\partial z \partial y} \right) + f_3 \left(\frac{\partial^2 u_x^{(i)}}{\partial x \partial z} + \frac{\partial^2 u_y^{(i)}}{\partial y \partial z} + \frac{\partial^2 u_z^{(i)}}{\partial x^2} + \frac{\partial^2 u_z^{(i)}}{\partial y^2} \right) = 0. \tag{9}$$

The coefficients f_1, f_2, f_3, and f_4 are as follows

$$f_1 = \frac{E_{(i)}(1-\nu_{(i)})}{(1+\nu_{(i)})(1-2\nu_{(i)})}, \quad f_2 = \frac{E_{(i)}\nu_{(i)}}{(1+\nu_{(i)})(1-2\nu_{(i)})},$$
$$f_3 = \frac{E_{(i)}}{2(1+\nu_{(i)})}, \qquad f_4 = \frac{E_{(i)}(1+\nu_{(i)})}{(1+\nu_{(i)})(1-2\nu_{(i)})}, \tag{10}$$

where the components of the displacement vector are denoted by u_x, u_y, and u_z [m]. Other variables used in the above equations include E [N/m^2] for Young's modulus, ν [-] for Poisson's ratio, a [K^{-1}] for the linear thermal expansion coefficient, and ΔT [K] for the temperature difference between the reference and current states, which is given by $\Delta T = T - T_{ref}$.

The global FEM equations for (1) and (7)–(9) are as follows

$$K_T^{(i)} \boldsymbol{T}_{f+1}^{(i)} + M_T^{(i)} \frac{\boldsymbol{T}_{f+1}^{(i)} - \boldsymbol{T}_f^{(i)}}{\Delta t} = \boldsymbol{B}_T^{(i)}, \tag{11}$$

$$K_D^{(i)} \boldsymbol{u}^{(i)} = \boldsymbol{B}_D^{(i)}, \tag{12}$$

where K_T represents the thermal conductivity matrix at a global scale, while M_T is the global thermal capacity matrix. Next, B_T corresponds to the global vector containing thermal boundary conditions, and $\boldsymbol{T}$ denotes the vector of unknown nodal temperatures at a particular time level f. Additionally, K_D is the global stiffness matrix, $\boldsymbol{B}_D$ is a vector of known boundary displacements, and $\boldsymbol{u}$ is the vector containing unknown nodal displacements.

3. Example of calculations

The mold is a rectangular prism with dimensions of $0.2 \times 0.2 \times 0.25$ m^3, while the casting is a prism of $0.1 \times 0.1 \times 0.2$ m^3. The mold is initially at a temperature of 400 K filled with the molten bronze of 1350 K. Convective heat transfer is specified on the external boundaries of the mold and on the top of the casting, with $\alpha = 100$ J/(s m^2 K) and an ambient temperature of 300 K. The time step remains constant at $\Delta t = 0.1$ s. Material properties of the mold-casting system are shown in Table I.

Thermal deformations in the casting during the cooling process are depicted in Fig. 2a–c, with magnifications of ten times for enhanced visibility. Notably, there is a significant reduction in the vertical dimension of the casting, accompanied by a gradual widening of the gas gap. At the end of the solidification process, which takes place after 135 s (see Fig. 2c), the average gap width is about 0.4 mm, while the vertical dimension of the casting decreases by approximately 1.5 mm.

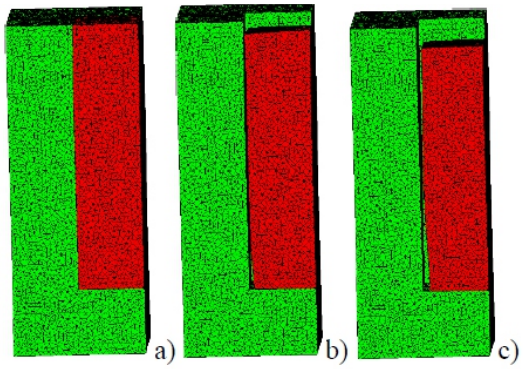

Fig. 2. Deformations of the casting (magnified 10x) at $t = 0$ s (a), $t = 60$ s (b), $t = 135$ s (c).

TABLE I

Material properties used in calculations.

Material property	Liquid phase	Solid phase	Mold	Air gap
λ	25	46	45	0.5
ρ	8300	8900	7200	–
c	540	440	753	–
ν	–	0.34	0.21	–
E	–	8.3×10^{10}	9.0×10^{10}	–
a	–	1.8×10^{-5}	0	–
T_L	1298		–	–
T_S	1243		–	–
L	2.2×10^5		–	–

4. Conclusions

The discussed model of solidification shows the impact of the air gap on casting cooling dynamics. Using separate meshes for the mold and casting saves operational memory by sequentially solving the equations. Future work will include the mechanical interaction of thermally deformed regions and account for radiation effects within the gap. Accurate prediction of gap location and width is crucial, especially for castings with complex boundaries.

References

[1] D. Mortensen, B.R. Henriksen, M. M'Hamdi, H.G. Fjær, in: *Essential Readings in Light Metals*, Eds. J.F. Grandfield, D.G. Eskin, Springer 2016, p. 812.

[2] L.A. Gowsalya, M.E. Afshan, in: *Casting Processes and Modelling of Metallic Materials*, Eds. Z. Abdallah, N. Aldoumani, London 2021, p. 41.

[3] W. Li, L. Li, Y. Geng, X. Zang, Y. Jing, D. Li, B.G. Thomas, *Metall. Mater. Trans. B* **52**, 2224 (2021).

[4] J. Xu, J. Kang, L. Zheng, W. Mao, J. Wang, *J. Mater. Res. Technol.* **19**, 2705 (2022).

[5] A. Chawla, N.S. Tiedje, J. Spangenberg, *Arch. Foundry Eng.* **23**, 53 (2023).

[6] T. Skrzypczak, E. Węgrzyn-Skrzypczak, L. Sowa, *Appl. Math. Comput.* **321**, 768 (2018).